NATIONAL OPTICAL ASTRONOMY OBSERVATORY

Preprint Series

NOAO Preprint No. 882

The Charge Transfer Efficiency and Calibration of WFPC2

Andrew E. Dolphin

(National Optical Astronomy Observatory)

To appear in: P.A.S.P. (October 2000)

June 2000

The Charge Transfer Efficiency and Calibration of WFPC2

Andrew E. Dolphin
National Optical Astronomy Observatories, P.O. Box 26372, Tucson, AZ 85726
Electronic mail: dolphin@noao.edu

ABSTRACT

A new determination of WFPC2 photometric corrections is presented, using HSTphot reduction of the WFPC2 Omega Centauri and NGC 2419 observations from January 1994 through March 2000 and a comparison with ground-based photometry. No evidence is seen for any position-independent photometric offsets (the "long-short anomaly"); all systematic errors appear to be corrected with the CTE and zero point solution. The CTE loss time dependence is determined to be very significant in the Y direction, causing time-independent CTE solutions (Stetson 1998; Saha, Lambert, & Prosser 2000) to be valid only for a small range of times. On average, the present solution produces corrections similar to Whitmore, Heyer, & Casertano (1999), although with an improved functional form that produces less scatter in the residuals and determined with roughly a year of additional data. In addition to the CTE loss characterization, zero point corrections are also determined as functions of chip, gain, filter, and temperature. Of interest, there are chip-to-chip differences of order 0.01-0.02 magnitudes relative to the Holtzman et al. (1995) calibrations, and the present study provides empirical zero point determinations for the non-standard filters such as the frequently-used F450W, F606W, and F702W.

Subject headings: techniques: photometric

1. Introduction

Shortly after the installation of WFPC2 on Hubble Space Telescope, it was discovered that the camera suffered from a charge transfer inefficiency, causing stars at the top of each chip to lose 10-15% of their charge while being read out. This effect was significantly reduced, although not eliminated, by cooling the camera from -76°C to -88°C. Holtzman et al. (1995, hereafter H95) gave initial estimates of the charge loss, and observed that it appeared to be related to the background level. Whitmore & Heyer (1997) quantified the

background dependence, and also detected a count dependence. Furthermore, a charge transfer loss was also seen in the X direction, which was also characterized by Whitmore & Heyer (1997).

A further complication arose when it was discovered that the Y and possibly X losses were growing with time, a dependence characterized by Whitmore (1998) and most likely caused by radiation damage. The most recent paper on this topic from the STScI WFPC2 group is Whitmore, Heyer, & Casertano (1999, hereafter WHC99), who combine the two earlier results and have a longer time baseline (through February 1999) with which to determine the time dependence.

In addition to these studies, there have been two recent independent determinations of the CTE loss. Stetson (1998, hereafter S98), using DAOPHOT reduction of the Omega Cen and NGC 2419 calibration fields, derived a calibration that produced similar results to Whitmore & Heyer (1997) but finding no significant time dependence (+0.0012 magnitudes per year for the typical star). Saha, Lambert, & Prosser (2000, hereafter SLP00), in a paper detailing errors in DoPHOT Cepheid reductions, found significantly different results from previous studies in their reductions of the NGC 2419 field: no detectable XCTE loss and no count dependence of the YCTE. The presence of very different conclusions as to the dependencies of the CTE loss leads to the uncomfortable possibility that the amount of the CTE loss is package-dependent, as aperture photometry, DAOPHOT, and DoPHOT reductions have produced different results. As one would hope that the stellar brightnesses scale linearly from package to package, the most likely cause of such a dependence would be in the background calculation. DoPHOT backgrounds, especially, contain a significant amount of starlight and thus it is possible that the lack of an obvious count dependence in the DoPHOT CTE solution was caused by the presence of a count dependence in the background level.

In addition to the CTE effect, a position-independent charge loss was detected and dubbed the "long-short anomaly" because it was first seen as a difference in the magnitudes of a star in short and long exposures. Casertano & Mutchler (1998, hereafter CM98) determined this effect to be a function of the number of counts rather than the exposure time through an analysis of the NGC 2419 calibration field, and determined a correction formula. SLP00 found evidence of such a position-independent correction in their F814W observations of the same data, but not in the F555W observations. S98 found no evidence of a position-independent anomaly in any of his data, despite also using the NGC 2419 calibration data.

Finally, the validity of the H95 calibrations have been called into question by a number of studies. In addition to the "long" zero points measured by Kelson et al. (1996), Saha et

al. (1996), Hill et al. (1998), and others, which were all about 0.05 magnitudes fainter than the H95 zero points, S98 and SLP00 have determined zero point corrections using their CTE solutions.

This paper uses HSTphot (Dolphin 2000) reductions of the Omega Centauri and NGC 2419 standard fields in an attempt to address the unresolved issues from the studies mentioned above. At the very least, should the CTE loss be determined to be package-dependent, it will be necessary to provide a solution that is valid for HSTphot reductions. However, a unified explanation of the different effects is preferred and will be sought. This study also provides something of a "trial by fire" for HSTphot, given the large amount of data (over 1000) images that were reduced, primarily non-interactively.

2. Observations and Reduction

As with S98, this study was based on observations of the Omega Cen and NGC 2419 calibration fields. The Omega Cen data comprise the bulk of the observations and span a wide baseline of epoch (January 1994 through March 2000), use all of the non-UV filters, and contain observations at both gain settings and both temperatures. However, nearly all of these data contain little or no background, so the NGC 2419 field (also used by S98 and SLP00) was added to improve the background baseline.

2.1. Ground-based Data

The ground-based Omega Cen data were those of Walker (1994), with stars fainter than V=21.0 eliminated because of the large scatter in the data at the faint end. The ground-based NGC 2419 data were provided by Peter Stetson, in which a similar faint-end cut had already been made. The faint cuts in both data sets, in addition to reducing the amount of low-quality data in the fits, avoid the photometry bias that is found just above the cutoff. As the WFPC2 data are generally deeper than the ground-based data, they also avoid this effect.

Given the superior resolution of HST over ground-based telescopes, it is not surprising that many of the ground-based stars were resolved into multiple star systems when observed by HST. In order to eliminate errors from this effect, all WFPC2 stars that fell within 0.8 arcsec of the ground-based standard star were combined into a single star. If the combined magnitude was more than 0.05 magnitudes brighter than that of the brightest constituent star, the standard star was thrown out. Otherwise, the star was kept, with the combined

magnitude used for the WFPC2 magnitude in the analysis. If at least 25% of all images with detections of a star contained bright companions, the star was eliminated from the analysis altogether. (In other cases, it was assumed that a cosmic ray was responsible for the second detection, as no cosmic ray cleaning could be made.) In this process, 29 Omega Cen stars and 13 NGC 2419 stars were eliminated.

For the remaining stars, the expected WFPC2 flight system magnitudes were calculated using the H95 zero points and color terms with the equation

$$\mathrm{WFPC2} = \mathrm{SMAG} + Z_{FG} - ZFS - T_{1,FS}\mathrm{SCOL} - T_{2,FS}\mathrm{SCOL}^2, \quad (1)$$

where the values are defined as in H95. For this analysis, it is assumed that the color terms from H95 are correct, a necessary assumption given that these data do not contain a range of colors sufficient to re-calibrate the color terms. However, filter-dependent corrections are determined for the zero points.

2.2. WFPC2 Data

WFPC2 observations of the Omega Cen and NGC 2419 standard fields were obtained from the STScI archive, using on-the-fly calibration to process the images using the best available calibration data at the time of retrieval. The Omega Cen data consist of 795 images, mostly in the standard filters (117 F439W, 271 F555W, 88 F675W, and 235 F814W), with additional images reduced but discarded because of insufficient overlap with the ground-based field. Additionally, data in secondary filters were also obtained (8 F380W, 8 F410M, 4 F450W, 6 F467M, 9 F547M, 7 F569W, 13 F606W, 2 F622W, 9 F702W, 7 F785LP, 2 F791W, 2 F850LP, and 4 F1042M). U observations, although available, were omitted because of the lack of ground-based comparison photometry in the Walker (1994) data.

The NGC 2419 data consist of 51 images (7 F555W and 44 F814W). F300W images were also available for NGC 2419, but were omitted in this analysis due to the lack of interest in calibrating F300W (as per the recommendation of H95). In the interest of producing the best possible calibrations, the chips containing NGC 2419 itself (WFC4 for five of the images; WFC2 for the remainder) were omitted from the analysis because of the higher crowding. This caused a mean magnitude offset of $\sim$0.02 magnitudes, which is reasonable in crowded field photometry but undesirable in a calibration study, especially since the NGC 2419 data provide most of the high-background points.

Photometry was made using the usual HSTphot recipe, except that cosmic ray cleaning was omitted because the images were reduced individually. Aperture corrections were made

to correct to the 0.5 arcsec aperture of H95. In order to reduce the number of bad points in the analysis, all stars were required to have $\chi \leq 1.5$ and $-0.3 \leq sharpness \leq 0.3$ to be used in the calibration solution. Additionally, all stars near the WFPC2 saturation limit were removed, as were stars with fewer than 105 electrons, which contributed more noise than signal to the solution. In all, 843 images were used for the solution, producing a total of 58728 cleanly-fit stars that were matched to the standard stars.

2.3. Background

As noted in Section 1, the most likely explanation of the apparent package dependence of the CTE loss is that different photometry packages calculate the background differently. Specifically, any package that determines a background level close to the star will invariably measure the wings of the star as part of the background. The DoPHOT sky measurement, as made by Saha et al. (1996) and SLP00, is perhaps the most severe example of this effect, with its average sky pixel containing ~0.2% of the star's total light. HSTphot, which also determines sky values near the star (although not as close as DoPHOT), shows this dependence at a smaller level.

In an attempt to create as generally useful a CTE determination as possible (as well as to provide independent parameters for the solution), the count dependence of the background was solved and subtracted from the background levels before running the calibration solution. Because the background contamination is proportionally the most significant at low background levels, it was calculated using the low-background Omega Cen data only.

This dependence was determined to be chip-dependent, in that it was about an order of magnitude smaller in PC1 but the same in the three WFCs, wavelength-dependent (smallest for B and V), and temperature-dependent (slightly larger at cold temperature than at warm temperature). The correction equations and coefficients are not given here, since this result almost certainly will not apply to other software packages. For example, DoPHOT background levels have a factor of $\sim$ 20 greater dependence on the number of counts than do HSTphot background levels.

Finally, as a negative background is a non-physical result of readout noise or bias errors on a very small background, all negative values were set to zero. The background and counts were converted to electrons by multiplying by the gain (7 or 14), and the background then softened according to S98's procedure (background = $\sqrt{1 + N_{electrons}{}^2}$) to allow logarithms to be taken at zero background. For the remainder of this paper, *counts*

will refer to the number of electrons detected for a star, while *background* will refer to the background level in electrons, so that the value of the gain is unimportant. If discussing values in DN rather than electrons, it will be made explicit.

3. Characterization

Before determining the CTE and zero point solution, some preliminary work needed to be done in order to constrain the form of the solution. It should be stressed that the constraints determined in this section are empirically determined from observed differences between WFPC2 and ground-based data, rather than based on any assumed physical model of the charge loss.

3.1. Position-Independent Corrections

The nature of the data in this present study - WFPC2 photometry with comparison ground-based photometry - permits a more direct study of the position-independent error ("long-short anomaly") than what was given by CM98. The complete sample of 58728 stars was restricted to points with limited ranges of counts, background, and epoch, thus producing a relatively homogeneous data set that should have a common set of correction factors. To maximize the ability to determine the position-independent correction, the *counts* were restricted to between 210 and 350, for which the average position-independent correction (based on CM98) should be about 0.23 magnitudes. The *background* was required to be 3.5 or less, which would include the greatest amount of data. The differences between WFPC2 and ground-based magnitudes were then fit to the formula

$$\Delta mag = c_0 + c_1 \frac{y}{800} + c_2 \frac{x}{800} + \Delta ZP. \quad (2)$$

($\Delta counts$ could have been used equally well, as the next section demonstrates, with the same result produced.) ΔZP is the zero point correction from Section 4, and is of order 0.01-0.02 magnitudes, depending on filter and chip. (In the initial solution, the ΔZP term was omitted, producing a result less than 0.01 magnitudes different from the one below. However, to minimize systematic errors, the term was added and the solution redone after running the CTE solution.)

A robust fit parameter was minimized using the nonlinear minimization routine *dfpmin* from Numerical Recipes in C (Press et al. 1992), providing the best values of the three parameters, and uncertainties estimated via bootstrap tests. In the solution, c_1 and c_2 are the YCTE and XCTE terms, respectively, while c_0 is the position-independent offset.

For the NGC 2419 data that were used by CM98, 21 stars were found that met the count and background criteria, producing a c_0 value of 0.02 ± 0.07 magnitudes. Expanding the sample to all 1997 data to improve the statistics, c_0 was determined to be 0.04 ± 0.05 magnitudes. To further improve the statistics, the count range was changed to $350 - 700$, producing 114 points and a correction of -0.01 ± 0.02 magnitudes despite the expected value of 0.12 magnitudes from the CM98 correction.

Although the uncertainties are significant, a position-independent offset of 0.23 magnitudes in the faint data is ruled out at almost the 4σ level, while the expected correction of 0.12 magnitudes for brighter points is ruled out at more than the 5σ level. Both samples, however, are consistent to well within 1σ with no anomaly, and therefore the CTE analysis below does not include a position-independent correction except for the zero point corrections, ΔZP. Further discussion of the long-short anomaly is given in Section 5.3.

3.2. CTE Functional Form

With the result of no position-independent correction, the functional form of the charge loss will include only XCTE and YCTE corrections. The first issue to be determined is whether the charge loss is of the form

$$\Delta counts = \frac{Y}{800}\mathrm{YCTE} + \frac{X}{800}\mathrm{XCTE} \tag{3}$$

or

$$\Delta magnitude = \frac{Y}{800}\mathrm{YCTE} + \frac{X}{800}\mathrm{XCTE} \tag{4}$$

As is demonstrated in Figure 1, which shows both magnitude residuals and the ratio of counts lost as a function of Y for a subset of the data, the choice of functional form does not make a significant difference. However, the plot as a function of magnitude difference gives the slightly better fit, so the form given in Equation 4 will be used for this study.

The CTE loss is assumed to depend only on counts, background, temperature, and epoch. This assumption was tested by determining the CTE solution for subsets of the data restricted by chip, gain, and filter. These subset CTE determinations produced corrections that were not significantly different from the full solution, thus verifying the assumption.

Finally, a number of numerical and observational criteria were set out, which the CTE functional form must satisfy.

- There must be no combination of counts, background, and epoch that would cause

the formula to become undefined.

- As the CTE effect is one of lost charge, the correction must never be negative.
- The logarithms of the mean magnitude residuals appear to scale roughly linearly with the logarithms of *counts* and *background*, implying a form involving $e^{c_{ct}\ln(counts)}$ and $e^{c_{bg}\ln(background)}$.
- A sufficiently high background will eliminate the CTE loss. For example, stars with less than 1000 *counts* and more than 1000 *background* have an average offset of -0.001 ± 0.015 magnitudes.
- A sufficiently high count rate will reduce but not eliminate the CTE loss. For example, stars with over 21000 *counts* but under 10 *background* have an average offset of 0.031 ± 0.001 magnitudes.
- A sufficiently early time will again reduce but not eliminate the CTE loss. For example, the average cold camera offset in 1994 is 0.020 ± 0.001 magnitudes.
- High count rates do not eliminate the time dependence, nor do early epochs eliminate the count dependence. For example, stars with 21000 or more *counts* increase from an average offset of 0.018 ± 0.002 to 0.041 ± 0.004 magnitudes from 1994 to 2000. Likewise, the 1994 correction increases from 0.018 ± 0.002 magnitudes for stars with at least 21000 *counts* to 0.083 ± 0.002 magnitudes for those between 500 and 1000 *counts*.

These observations restrict the set of functional forms that can be used. Attempts were made to adopt different forms obeying the above restrictions, with the formulae below producing the best fits to the data.

$$yr = epoch - 1996.3 \tag{5}$$

$$lct = \ln(counts) - 7 \tag{6}$$

$$lbg = \ln(background) - 1 \tag{7}$$

$$\mathrm{YCTE} = \frac{Y}{800}\left[\, y_0 + (y_1 + y_2 yr)(y_3 + e^{-y_4 lct})e^{-y_5 lbg - y_6 bg} \,\right], \tag{8}$$

$$\mathrm{XCTE} = \frac{X}{800}\left[\, (x_1 + x_2 yr)e^{-x_4 lct - x_5 lbg} \,\right]. \tag{9}$$

The offsets of 1996.3, 7, and 1 were roughly the averages of these values in the data, and were included to improve numerical stability and to produce independent coefficients.

(Failing to do so would have provided correlated coefficients and thus correlated errors.) The addition of the y_6 parameter was required to eliminate an overcorrection at moderate and high background levels seen in the first solution. No similar x_6 parameter was needed. Additionally, x_0 and x_3 terms analogous to the y_0 and y_3 terms were initially included but were determined to be insignificant (well less than 1σ) and subsequently removed from the equation.

Note that in the above functional form, all coefficients y_i and x_i must be positive to meet the requirements itemized above. Additionally, to avoid negative corrections at early epochs (1994.3), y_1 must be at least twice y_2 and likewise for x_1 and x_2.

Separate sets of constants were determined for the warm (−76°C) and cold (−88°C) camera observations. However, all warm camera observations were made with little or no background and at similar time (January through April 1994), so no background or time dependence could be determined. Additionally, no XCTE loss was measurable in the warm data.

3.3. Zero Point Corrections

In addition to the CTE solution, a set of zero point corrections was also determined. The first correction was made to search for any offset between the ground-based Omega Cen and NGC 2419 data. This correction factor was determined to be well under 0.01 magnitudes (and less than a 1σ effect), and was eliminated.

The remaining corrections, as functions of filter, temperature, chip, and gain, were divided into two sets. This division, though made primarily for numerical reasons, was not entirely arbitrary. The "ideal" solution would naturally involve a zero point correction for every combination of temperature, filter, chip, and gain, or a total of 272 free parameters. This total was reduced to 25 by adopting the following assumptions and simplifications:

- The principal factors affecting detection efficiency are wavelength and temperature. This makes the assumption that the four chips have similar wavelength-dependent quantum efficiencies (an overall sensitivity difference would be corrected by item 3 in this list), which was verified by determining the CTE corrections individually for the four chips. This creates 34 filter- and temperature-dependent zero point offsets.

- Although the non-standard filter offsets are temperature-dependent, the differences between their corrections and the corrections of the standard magnitudes of the same color are observed to be independent of temperature. This allows the consolidation

of the 26 non-standard filter zero point corrections to 13 corrections relative to the nearest standard filter, and the reduction of the 34 total temperature/filter zero point offsets to 21.

- The principal factors in the readout efficiency are chip and gain setting, as each of the eight combinations involves slightly different electronics. This creates 8 zero point offsets dependent on chip and gain. After running the solution, it was determined that the gain setting made no measurable difference, further reducing these offsets to 4.

Thus the total zero point correction is thus

$$\Delta ZP = \Delta ZP_{T,color} + \Delta ZP_{filter} + \Delta ZP_{chip}. \quad (10)$$

As with the CTE loss correction, all of the zero point corrections were computed in the sense that they should be subtracted from the WFPC2 magnitudes to produce standardized magnitudes.

4. CTE and Zero Point Solution

The solution for the CTE effect and zero point corrections was made by iteration. The program was a more sophisticated version of that used to determine the position-independent correction in section 3.1. In order to produce an adequate fit parameter, it was necessary to add 0.02 magnitudes (in quadrature) to the uncertainty of every point. The source of this additional uncertainty is unknown, and was also noticed by S98. After the solution, all photometry was re-read, with corrected points falling more than 0.15 magnitudes and 2σ away from the standard magnitudes removed for the next iteration. This process continued until the same points were removed for consecutive iterations. For the final iteration, 55910 of the 58728 points were used.

4.1. CTE Coefficients

The final coefficients and offsets provide the values to subtract from the observed WFPC2 magnitudes (calibrated using H95 flight system zero points, gain ratios, and pixel area ratios) to generate corrected WFPC2 flight system magnitudes. The CTE coefficients are given (with 68% confidence limits) in Tables 1 and 2 for cold and warm data, respectively. As noted above, no XCTE loss was detectable in the warm camera

observations, but can be characterized well in the cold observations. The time dependence of the cold XCTE loss is small and is consistent with the Whitmore (1998) time dependence, while the dependence on counts is much higher than that on background. The detection of any significant background dependence in the XCTE loss is different from S98 and WHC99, but the effect on the corrections is minimal given the size of the XCTE correction. The XCTE loss is only a minor effect, with the worst-case combination in the calibration data ($lct = -1.15$; $bg = 1$, $lbg = -1$; $yr = 4$) producing an XCTE ramp of only 0.05 magnitudes.

The YCTE loss is by far the larger of the two. The primary difference between warm and cold is the YCTE base value y_0, which decreased by 0.08 magnitudes when the instrument was cooled. As opposed to the XCTE equation, the YCTE loss is strongly dependent on counts, background, and time. Again the time dependence is consistent with the values from Whitmore (1998). The worst-case combination will produce a YCTE ramp of 0.50 magnitudes, consistent with the WHC99 result of a $\sim$ 40% loss for faint stars on low background in early 1999.

A second simple check can be made by determining the corrections for the conditions used by H95 ($lct = 1$; $bg = 3$, $lbg = 0$; $yr = -1.8$) to determine their corrections of 0.10 to 0.15 magnitudes in the warm data and 0.04 in the cold. These values lead to YCTE ramps of 0.11 magnitudes in the warm data and 0.03 magnitudes in the cold data, consistent with the H95 CTE loss estimates. Detailed comparisons with the recent studies are given in Section 5.2.

4.2. Zero Point Offsets

The zero point offsets by color and temperature are given in Table 3. There is a clear trend of increasing offset with increasing wavelength for the cold data, and the opposite case in the warm data. This trend was extrapolated to U (F336W) to compensate for the lack of U data in the calibration sample. Because of the extrapolation, the uncertainties are likely $\sim$0.01 magnitudes. The cause of these offsets is unknown, as the H95 calibrations were based on these same set of observations. Systematic differences between HSTphot and aperture photometry are unlikely, especially given the excellent agreement between the present CTE loss determination and that by WHC99. It is also not a time-dependent effect, as this trend is still seen if only the 1994 data are used. The easiest explanation would be that H95 used both warm and cold data, as the offsets would roughly cancel out if added, but this was not the case. Compared with the synthetic zero points of Table 28.1 of the HST data handbook, the new zero points are on average 0.02 magnitudes fainter, with RMS scatter of 0.02 magnitudes. The difference is most likely the result of the handbook

zero points, which are only claimed to be accurate to 0.02 magnitudes.

Table 4 gives the zero point corrections of the non-standard filters, which should be subtracted from the observed WFPC2 flight system magnitudes in order to determine magnitudes on the same system as the standard filter of the same color. (In addition, The Table 3 value should be subtracted to produce magnitudes corrected to the ground-based data.) It is assumed that these values are nonzero because the H95 transformations for these filters were synthetic rather than empirical, and thus were not directly tied to any observed system. Given the amount of observations made in F450W and F606W, it is worth noting that while the F450W magnitudes appear to be correct relative to F439W, F606W magnitudes are off by 0.02 magnitudes relative to F555W. A comparison between the new zero points and those in Table 28.1 of the HST data handbook indicates that the handbook zero points fare quite poorly, with RMS scatter of 0.08 magnitudes between the new zero points and those of Table 28.1 for the non-standard filters. In comparison, the RMS scatter between the new zero points and the synthetic zero points of H95 is less than half of that value.

Finally, the chip-to-chip zero point corrections are 0.037 ± 0.001, -0.012 ± 0.001, 0.007 ± 0.001, and 0.004 ± 0.001 for PC1, WFC2, WFC3, and WFC4, respectively. The presence of non-zero chip-to-chip differences implies either a minor error in the relative pixel areas reported by H95 or a sensitivity difference between the four chips. Although other studies have determined that chip-to-chip offsets are a function of filter as well as gain, such an effect is not observed here at any significant level.

4.3. WFPC2 Calibration Formulae

Rather than calibrating using H95, and then applying two or three sets of zero point corrections, it is simpler to apply the corrections to the calibration process. The calibration equations, analogous to equations 7 and 8 of H95 but incorporating the pixel area correction, would be

$$\mathrm{WFPC2} = -2.5\log(DN/s) + Z_{FG} + \Delta Z_{CG} - \mathrm{CTE} \tag{11}$$

and

$$\mathrm{SMAG} = -2.5\log(DN/s) + Z_{FS} + T_1\mathrm{SCOL} + T_2\mathrm{SCOL}^2 + \Delta Z_{CG} - \mathrm{CTE}. \tag{12}$$

ΔZ_{CG} is the zero point modification for chip and gain settings, and the values can be found in Table 5. Z_{FG} in Table 6, and Z_{FS}, T_1, and T_2 in Table 7, and follow the definitions of H95. The terms T_1 and T_2 in Table 7 are reproduced from Tables 7 and 10 of H95. The CTE correction should be calculated from Equations 5-9 and Table 1 for cold data or 2 for

warm data. Again, it should be noted that aperture corrections were made to the 0.5 arcsec aperture of H95 and others, rather than the nominal infinite aperture of the zero points in Table 28.1 of the HST data handbook.

5. Tests of the Corrections

5.1. Internal Consistency

Residuals (WFPC2 magnitude minus ground-based magnitude) from before and after applying the CTE correction and revised calibration are shown in Figures 2-5, plotted against Y, X, ln(*counts*), and ln(*background*), in order to provide a preliminary test of the correction formulae. As the figures demonstrate, the correction has been successful, at least to first order, in reducing the systematic residuals to under 0.01 magnitudes.

A concern in adopting any functional form for the corrections is that it will not properly account for second-order factors. For example, one frequently-mentioned concern is that the count dependence in the CTE corrections changes as a function of background level. This can be readily tested, with mean residuals for combinations of low and high counts, background, and epoch shown in Table 8. None of the residuals in the table are significantly more than 0.005 magnitudes.

However, the most significant source of concern is caused by the fact that the average calibration data are significantly different from most science data. The calibration observations are generally bright stars with little background (due to short exposure times), while most science observations are long enough to have a significant background and most projects require accurate photometry as faint as possible. The effect of this can be tested, and the solution appears to have succeeded despite these problems, with the average residual for points with *background* between 35 and 105 (typical for most science exposures) being 0.003 magnitudes.

Another potential source of error in the calibration is at the faint end, as there are insufficient stars in the calibration sample with < 350 *counts* (and those that are present naturally have large uncertainties) to have much effect on the solution. Therefore, the solution is largely extrapolated below 350 *counts* and subject to significant systematic errors. Such an effect can be checked by comparing the relative photometry of the NGC 2419 field, in a manner similar to that of CM98, but only using the F814W images with no preflash. The multiple image version of HSTphot, *multiphot* (Dolphin 2000), was used in order to reduce the random scatter and force a common object list. The 100 and 300 second images had sufficient background (at least 1 DN per pixel) to reduce faint sensitivity

and were omitted. As with the CTE study, the more crowded chip (WFC2) including the globular cluster was omitted to improve the photometry. Figure 6 shows the short (10- and 40-second exposure) magnitudes minus the 1000s magnitudes for these stars plotted against ln(*counts*) scaled from the 1000s image, before CTE correction in the top panel and after correction in the bottom. Only well-fit stars ($\chi \leq 2$ and $-0.3 \leq sharpness \leq 0.3$ are shown. No systematic error is detectable, aside from the effect of the photometry cutoff beginning around ln(*counts*) = 5.3, or 200 electrons. Between ln(*counts*) of 5.3 and 5.5, the median residual after CTE correction is -0.01 magnitudes, while the median uncorrected residual is 0.15 magnitudes. However, even down to ln(*counts*) = 4.9 (134 electrons), the mode of the distribution is within 0.01 magnitudes of zero, giving confidence in the photometry to the faintest level.

As a final check on the corrections, the corrected WFPC2 data were used to determine combined magnitudes of the Omega Cen and NGC 2419 standard stars. A comparison of ground-based and corrected WFPC2 data is given in Figure 7, showing good agreement.

5.2. Comparison with Previous CTE Studies

In order to make a comparison between the present corrections and those of S98, WHC99, and SLP00, all four sets of corrections were applied to the data set used in this study. To be perfectly fair, it should be noted that this study's corrections are at somewhat of an advantage, given that the same data used to determine the corrections are now used for the comparison. However, the data set used here is identical (although larger) than that used in the earlier studies, and the quality of the photometry should be at least as good as that in the earlier studies given the use of HSTphot. Finally, the fact that all major differences are attributable to obvious causes gives confidence that the comparisons are accurate.

To eliminate the effects of zero point differences, the present zero point corrections were applied to the WHC99 study, while the S98 and SLP00 zero points were applied respectively. In order to adequately model the SLP00 background dependence, their background parameter was modified for the observed DoPHOT count-background correlation

$$\text{DoPHOT background} = (\text{Dark Background}) + 2 \times 10^{-3} counts. \quad (13)$$

Residuals (corrected WFPC2 magnitudes minus standard magnitudes) are given in Table 9.

In terms of the overall corrections in the top line of the table, the WHC99 equations

produce very similar results to the present study. The S98 and SLP00 corrections are also reasonably good on average, but produce considerably more scatter. The cause of this extra scatter is clear when examining the remaining lines in Table 9: neither includes a time-dependent term and thus has a trend of increasing residual with time, in the sense that the 2000 data are significantly under-corrected in both studies. Since the WFPC2 magnitude of the average star in this data set has increased by 0.06 magnitudes from 1994 to 2000 (and that the magnitude of the average star with 350 electrons or less has increased by 0.18 magnitudes), it would have been surprising had either S98 or SLP00 been consistent with all of the available data.

A plot comparing the present CTE corrections to those of S98 using only cold F555W and F814W data obtained before 1997 and ignoring zero point differences is shown in Figure 8. The corrections clearly agree extremely well for this limited data set, with an average difference of 0.004 magnitudes and scatter of 0.015 magnitudes. However, the time dependence limits the usefulness of the S98 solution, with the 1999-2000 data producing an average difference of 0.061 magnitudes with significantly more scatter.

A similar comparison made with SLP00 is shown in Figure 9, using only F555W and F814W data obtained during 1997. The effect of the different functional form used for the two colors is apparent, with the F555W correction (which has no position-independent term) producing excellent agreement (under-correcting on average by 0.006 ± 0.010 magnitudes) while the F814W correction (which has a position-independent term) considerably off (over-correcting on average by 0.026 ± 0.025 magnitudes). Although the zero point offsets will compensate for this error in conditions identical to the calibration data used by SLP00, it is dangerous to assume that this will be the case in general.

Finally, the agreement between the present corrections and those of WHC99, shown in Figure 10 for data taken through February 1999, is excellent. Although the data show more scatter than Figure 8, a figure using the WHC99 corrections restricted to data before 1997 (as per Figure 8 would show only 65% the scatter. The differences become significant only at more recent epochs, where the WHC99 functional form (with the count dependence tied to the time dependence) begins to break down. For example, the average star with under 1000 counts observed between February 1998 and February 1999 has an average residual of 0.10 ± 0.14 magnitudes with the WHC99 corrections, while those of this study produce an average residual of 0.00 ± 0.10 magnitudes.

Thus the differences between the results of this study and previous recent studies can be explained fairly easily. Neither S98 nor SLP00 included a time effect, producing large deviations in corrections for stars beyond the times in which the data were taken. The remaining significant scatter between this study and SLP00 is due to the use of a single

parameter (the DoPHOT background level) instead of both the dark background and counts. Minor differences remain between all four corrections, due to different choices made in the functional forms.

This comparison of the different CTE solutions appears to explain the discrepancies, leading to the conclusion that, provided any count dependence is removed from the background levels, there is no package dependence in the CTE loss. It is thus suggested that the present CTE study, which contains a time dependence and corrects some of the shortfallings in the WHC99 functional form, should be applicable to all WFPC2 stellar photometry.

5.3. The Long-Short Anomaly Revisited

The previous section shows, reassuringly, that differences between previous CTE studies are primarily the result of assumptions of time dependence and the method of background calculation. However, the different results for the long-short anomaly (a position-independent charge loss) need to be reconciled as well.

Positive results regarding the detection of a long-short anomaly have come from the modified zero points of Saha et al. (1996), Kelson et al. (1996), and Hill et al. (1998), all of whom found that magnitudes from long exposures are about 0.05 magnitudes more than those from short exposures. CM98 characterized this effect, providing a correction formula that was based on the number of counts rather than the exposure time. However, S98 attempted to determine a position-independent loss in his CTE solution, but found no evidence for it, and Section 3.1 of this paper likewise finds no evidence. Finally, Section 5.1, which compares magnitudes from the 1000-second exposure of NGC 2419 with those from 10- and 40-second exposures, finds no effect at more than the 0.01 magnitude level.

In order to understand the nature of this effect, a more detailed comparison between the present data and that of CM98 needs to be made. Specifically, Figure 6 was taken from the same data used by CM98 and compared in the same way (short magnitude minus the 1000-second magnitude), and should thus be nearly identical to the 10s and 40s lines of Figure 11 of CM98 (although CM98 Figure 11 is plotted against short counts rather than scaled long counts). However, while CM98 shows a median short minus long error of 0.27 magnitudes for $\ln(counts) = 5.4$, the difference in this study is only -0.01 magnitudes. The difference between the two studies is also in the pre-CTE correction photometry, with Figure 9 of CM98 showing a magnitude difference of about +0.38 magnitudes and the top panel of Figure 6 showing a difference of +0.15 magnitudes at $\ln(counts) = 5.5$, thus ruling

out the CTE solution as the source of the anomaly.

The difference, then, appears to stem from the photometry. The most plausible explanation for the apparent long-short anomaly is an overestimate of the sky by CM98, as well as by previous authors. The expected functional form of the magnitude error caused by a sky measurement error is

$$\Delta mag = -2.5 \log(1 - \frac{\pi r^2 \Delta sky}{counts}), \tag{14}$$

where Δsky is the error per pixel in the sky value and *counts* is the number of counts. For the two-pixel radius used by CM98, a sky error of +0.58 DN or +4.1 electrons would match the CM98 correction formula to within 0.01 magnitudes for stars with detections of 33 DN or more. This potential solution to the problem would also explain the aperture dependence of the effect seen by CM98, as a larger aperture should be more susceptible to a sky error. Finally, this would explain why CM98 found only a count dependence in the short-long anomaly. This also would explain the Hill et al. (1998) remark that the effect appeared to be a constant subtraction of 2 electrons from every star pixel but not the background pixels, as a background overestimation would do exactly that.

In summary, there appears to be no convincing evidence for a long-short anomaly. It would be quite remarkable if a real effect of 0.27 magnitudes measured by CM98 was reduced to -0.01 magnitudes by an error in HSTphot; rather it is more likely that an error in the CM98 reduction was responsible for a false detection of the anomaly. Given the similarity between the CM98 correction equation and Equation 14 of this paper given Δsky error of 0.58 DN, which agree at the 0.01 magnitude level above 33 DN, as well as the simple explanation of the aperture dependence of the effect, the most probable cause of the CM98 result (as well as the other reports of the long-short anomaly) is an overestimation of the background by a few electrons.

6. Summary

An HSTphot-based CTE and zero point correction study, based on the Omega Cen and NGC 2419 observations, attempts to accomplish two goals. First is a comprehensive testing of HSTphot, which succeeded in reducing well over 1000 WFPC2 images without any problem. Given the tight agreement between this study and previous CTE work of S98 and WHC99, it seems that HSTphot is able to produce photometry without any noticeable systematic effects.

The more ambitious goals of this study were to improve upon existing CTE

determinations, and to determine the cause of differences between the previously published corrections. A functional form for the CTE correction was arrived at semi-empirically, and the coefficients were solved using an iterative nonlinear minimization process. The correction formulae were then applied to the observed data, resulting in no systematic residuals larger than 0.005 magnitudes. Additionally, the corrections were applied to relative photometry of the NGC 2419 field, with no significant errors found down to the faintest stars measured (under 140 electrons). New zero points were also determined for 18 of WFPC2's medium and wide filters, including empirical calibrations of the non-standard filters, such as F606W. These new zero points provide evidence of significant errors in the synthetic zero points given in the HST data handbook.

The corrections were also compared to those from previous studies (S98, WHC99, and SLP00). The major differences between the four sets of corrections are understandable in terms of the lack of a time dependence in S98 or SLP00 and the lack of a count dependence in SLP00. The primary difference between this study and WHC99 is the use of an improved characterization of the count and time dependencies. In terms of producing smaller systematic and random residuals over the full time baseline, the present set of corrections proved superior to all three other formulations, although the WHC99 CTE equations will also produce corrections accurate to a few hundredths of a magnitude in all cases except for recent (1998 and later) data with low counts. The previous detections and characterizations of the long-short error are believed to result from sky overestimation, an error which would cause the count dependence characterized by CM98 and fit their correction formula to within 0.01 magnitudes, as well as explaining the aperture dependence and lack of background dependence.

It is concluded that, given the understanding of the differences between this and other CTE studies, the present corrections should be valid for use on all WFPC2 stellar photometry, regardless of the photometry procedure, and are an improvement on previous work. However, due to differences in the determination of background (especially by DoPHOT), the contribution of starlight to the background level must be fit and removed in order to determine the dark background for a star.

I would like to thank Alistair Walker and Peter Stetson for providing the ground-based Omega Cen and NGC 2419 photometry, respectively. This work was supported by NASA through grants GO-02227.06-A and GO-07496 from Space Telescope Science Institute.

REFERENCES

Casertano, S., & Mutchler, M. 1998, WFPC2 Instrument Science Report 98-02 (CM98)

Dolphin, A. E. 2000, PASPsubmitted

Hill, R. J. et al. 1998, ApJ, 496, 648

Holtzman, J., Burrows, C. J., Casertano, S., Hester, J. J., Trauger, J. T., Watson, A. M., & Worthey, G. 1995, PASP, 107, 1065 (H95)

Kelson, D. D. et al. 1996, ApJ, 463, 26

Press, W. H., Teukolsky, S. A., Vetterling, W. T., & Flannery, B. P. 1992, *Numerical Recipes in C: The Art of Scientific Computing*, Second Edition, Cambridge: Cambridge University Press, pp. 425-430

Saha, A., Labhardt, L., & Prosser, C. 2000, PASP, 112, 163

Saha, A., Sandage, A., Labhardt, L., Tammann, G. A., Macchetto, F. D., & Panagia, N. 1996, ApJ, 466, 55 (SLP00)

Stetson, P. B. 1998, PASP, 110, 1448 (S98)

Walker, A. R. 1994, PASP, 106, 828

Whitmore, B. 1998, WFPC2 Technical Instrument Report 98-01

Whitmore, B. C., & Heyer, I. 1997, WCPC2 Instrument Science Report 97-08

Whitmore, B., Heyer, I., & Casertano, S. 1999, PASP, 111, 1559

This preprint was prepared with the AAS LaTeX macros v4.0.

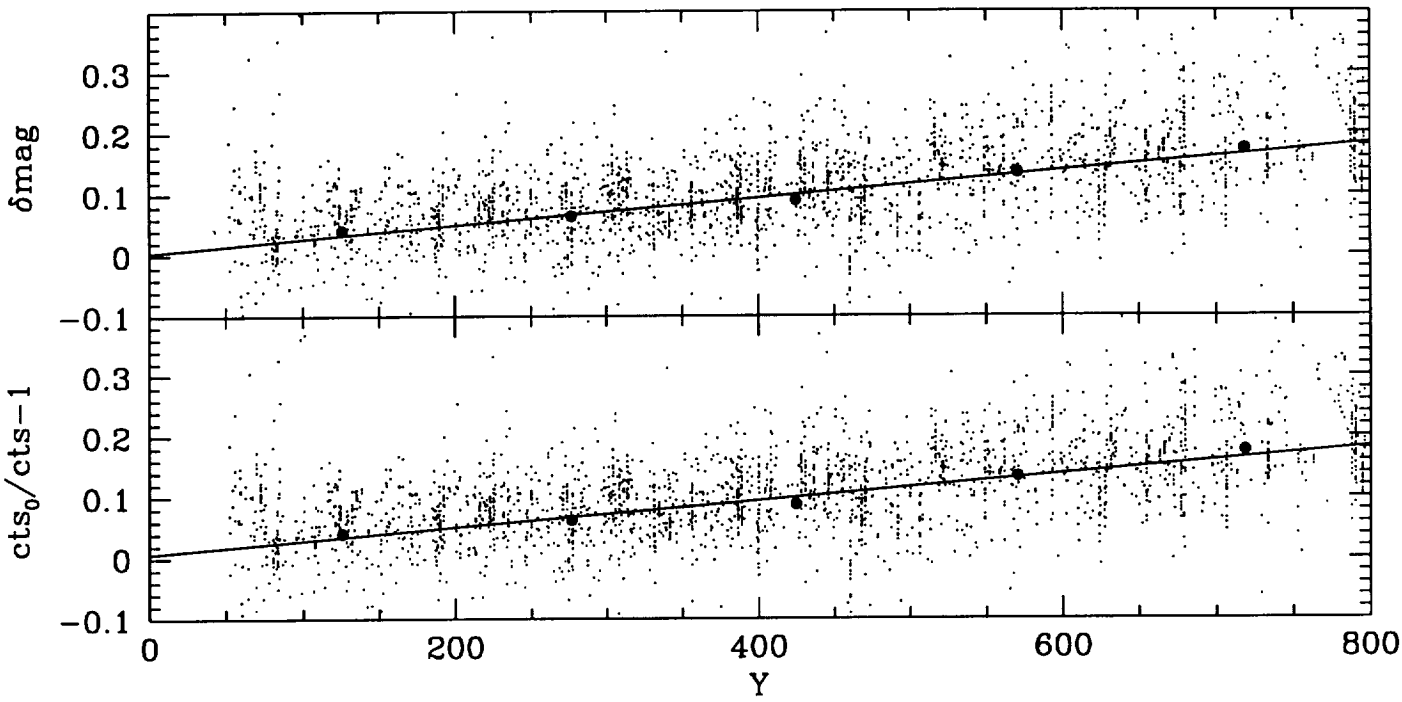

Fig. 1.— Charge loss and magnitude loss as a function of Y for a subset of the data. The heavy dots are the average values.

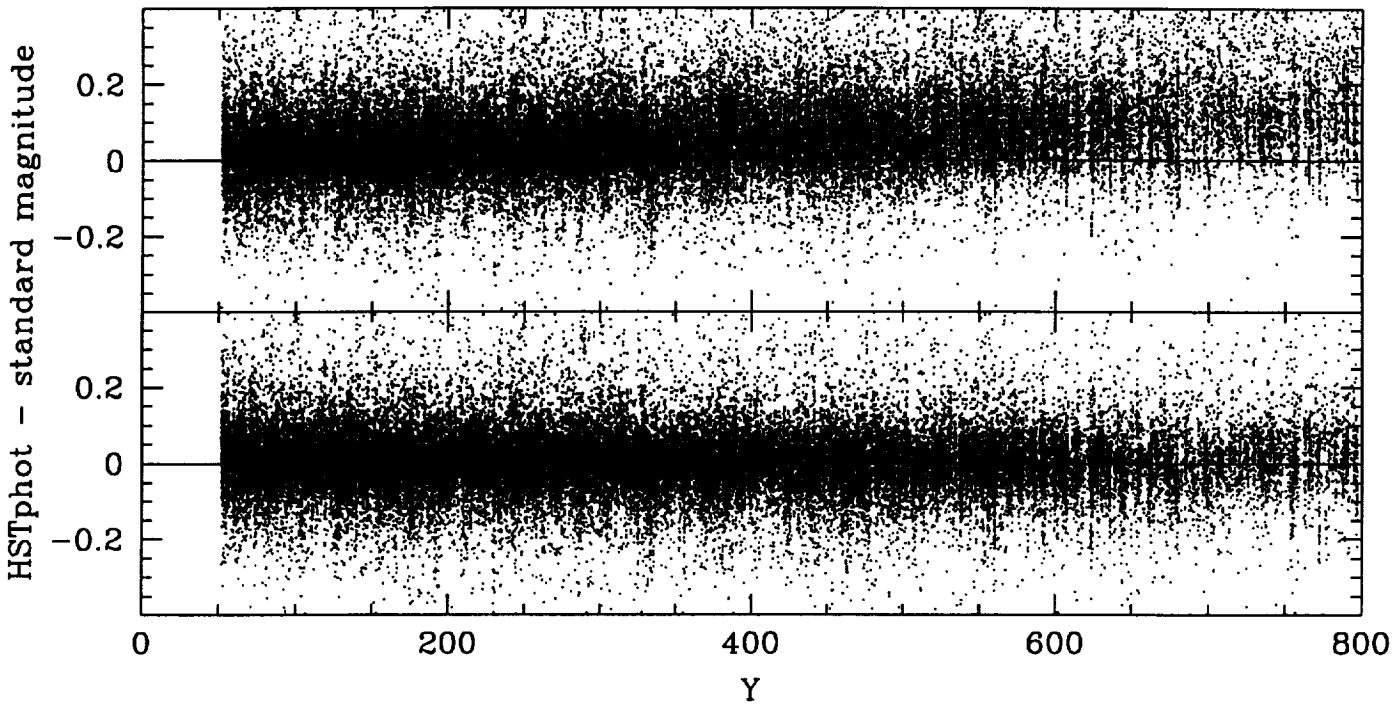

Fig. 2.— CTE effect before (above) and after (below) correction, plotted against Y

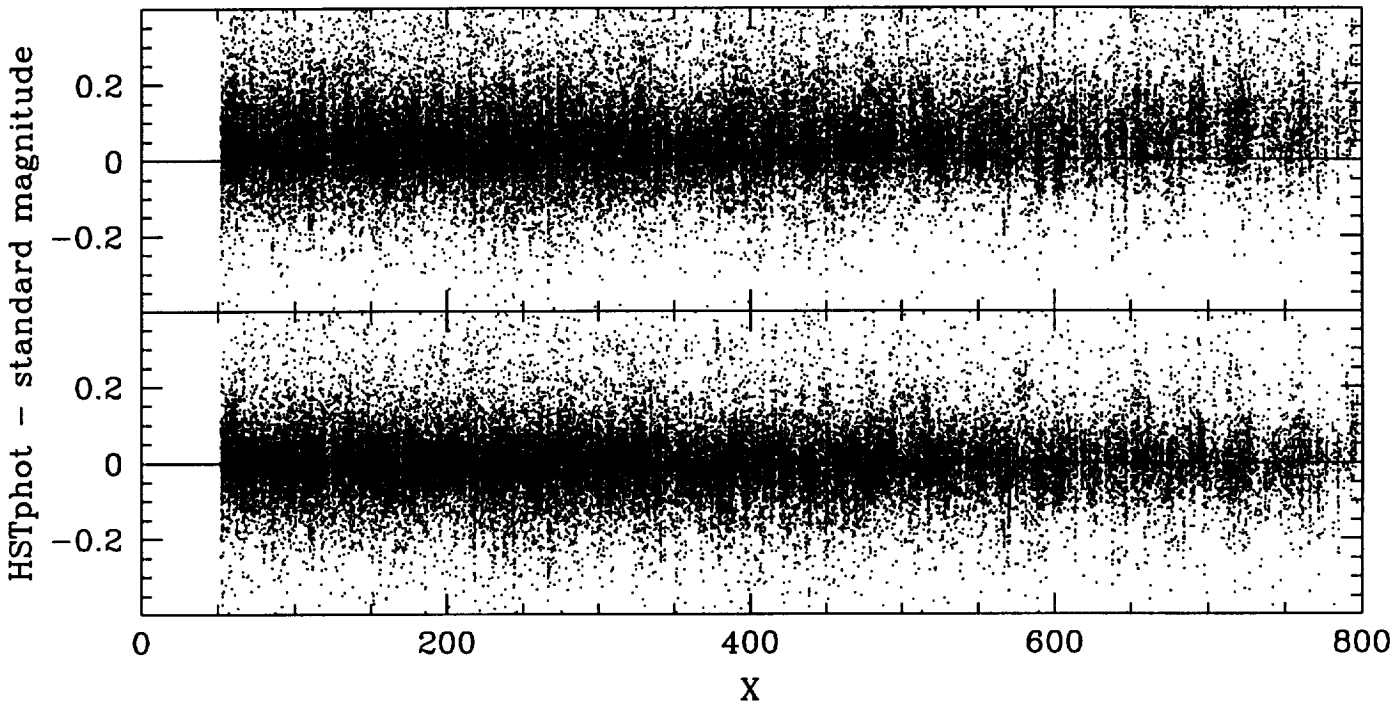

Fig. 3.— CTE effect before (above) and after (below) correction, plotted against X

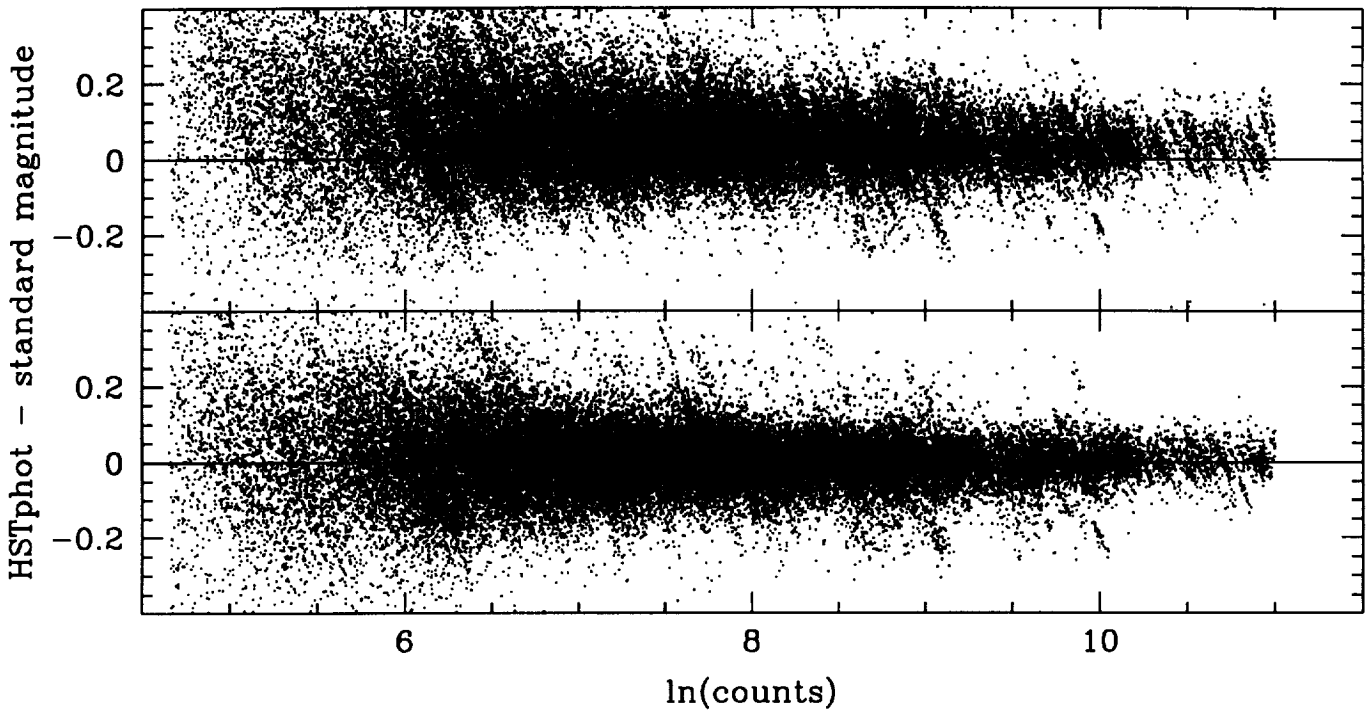

Fig. 4.— CTE effect before (above) and after (below) correction, plotted against ln(*counts*)

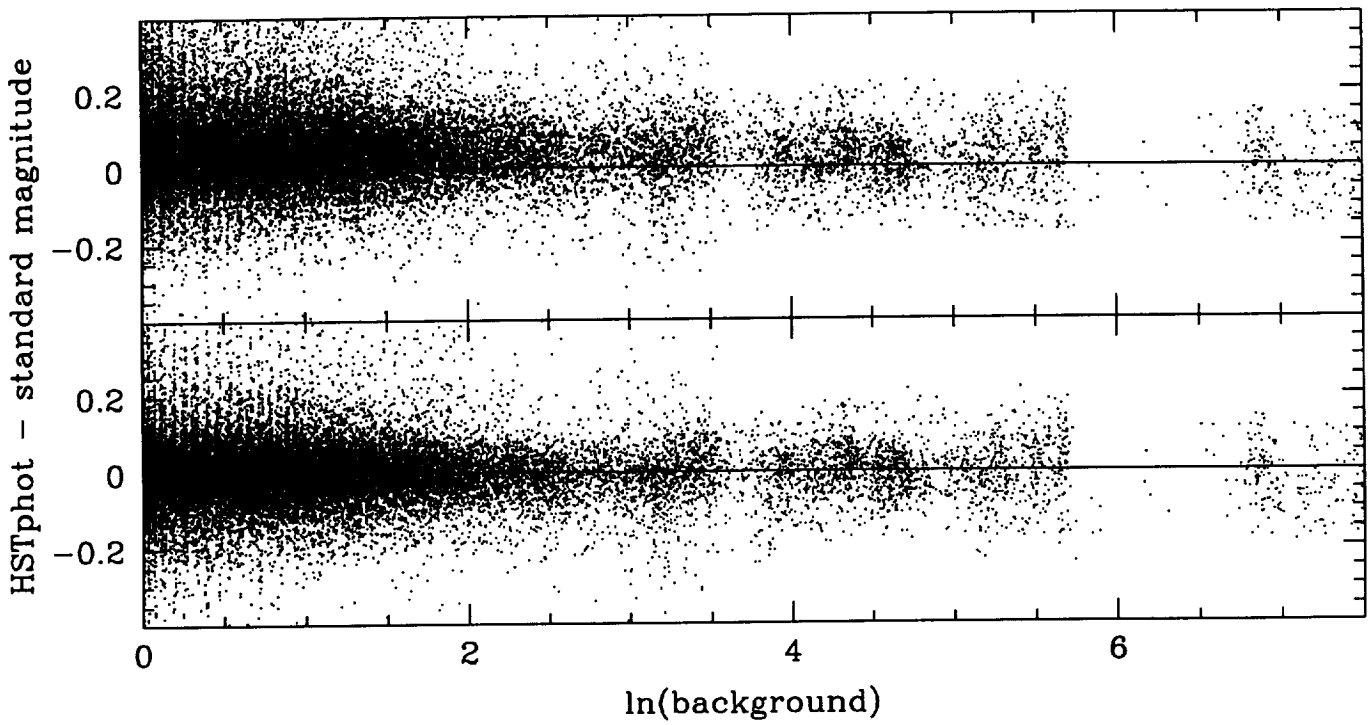

Fig. 5.— CTE effect before (above) and after (below) correction, plotted against ln(*background*)

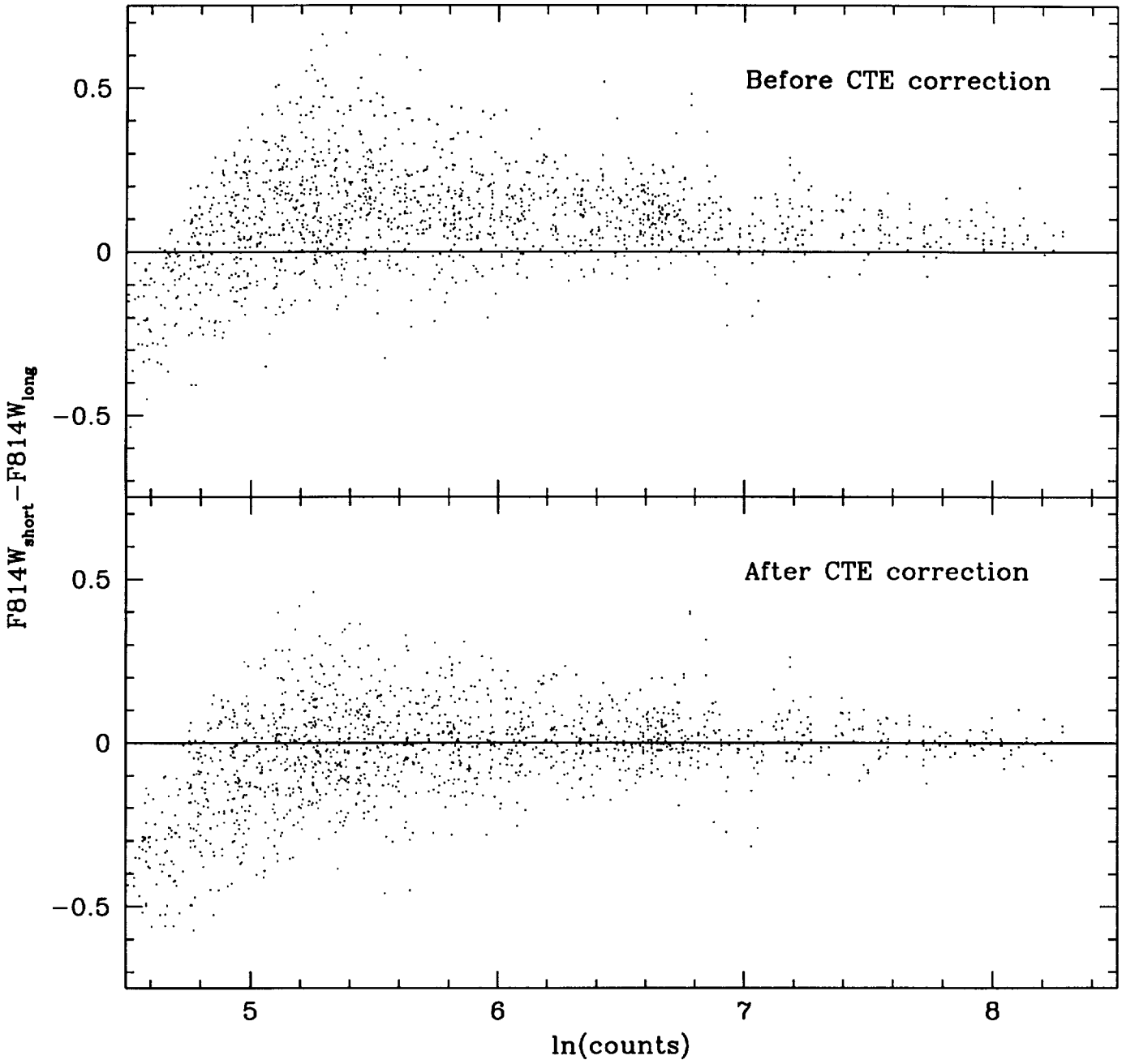

Fig. 6.— NGC 2419 F814W relative photometry, with short minus long magnitudes for zero preflash 10- and 40-second images plotted against the number of counts.

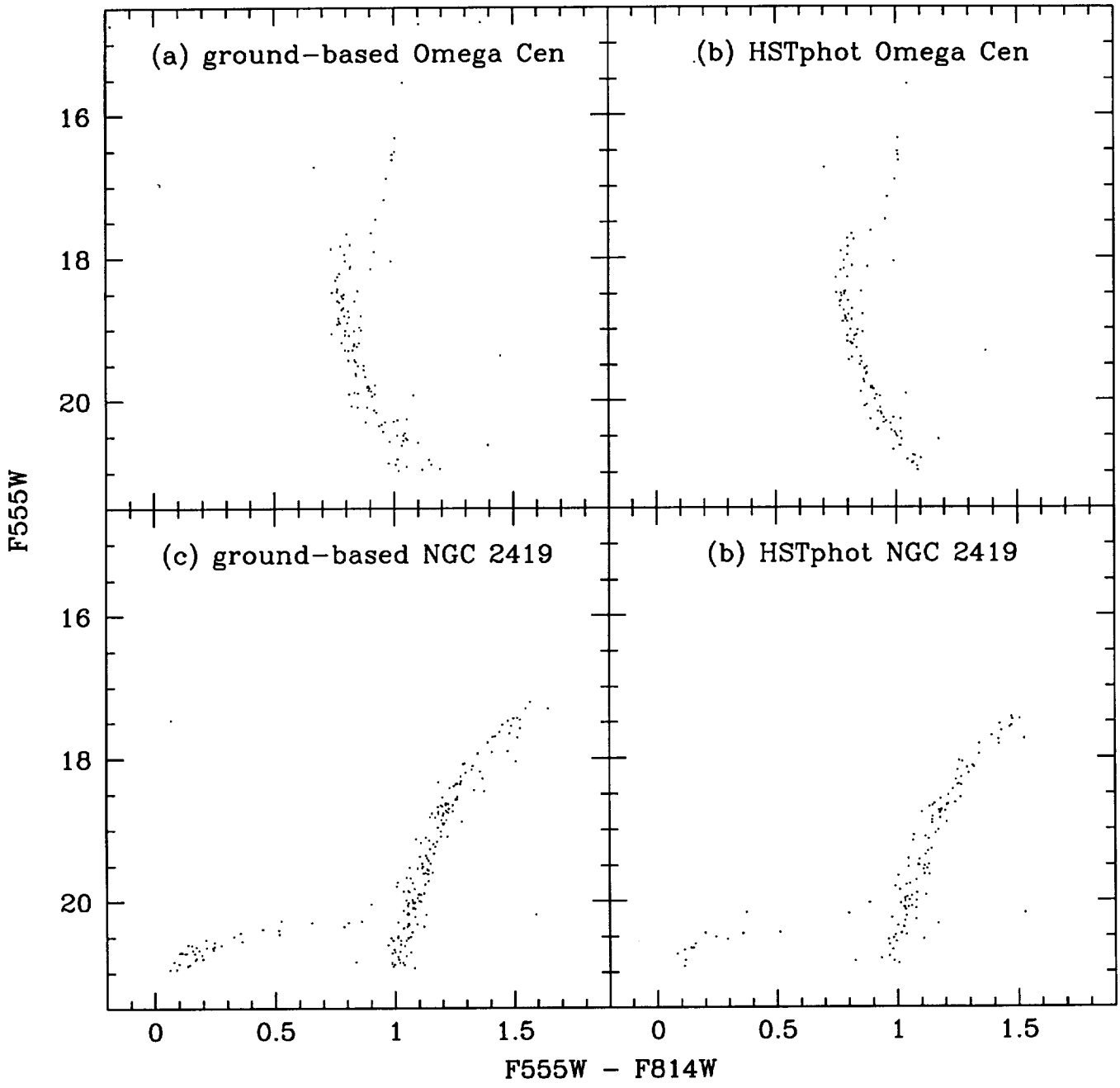

Fig. 7.— Omega Centauri and NGC 2419 photometry, with ground-based data in (a) and (c) and calibrated HSTphot data in (b) and (d)

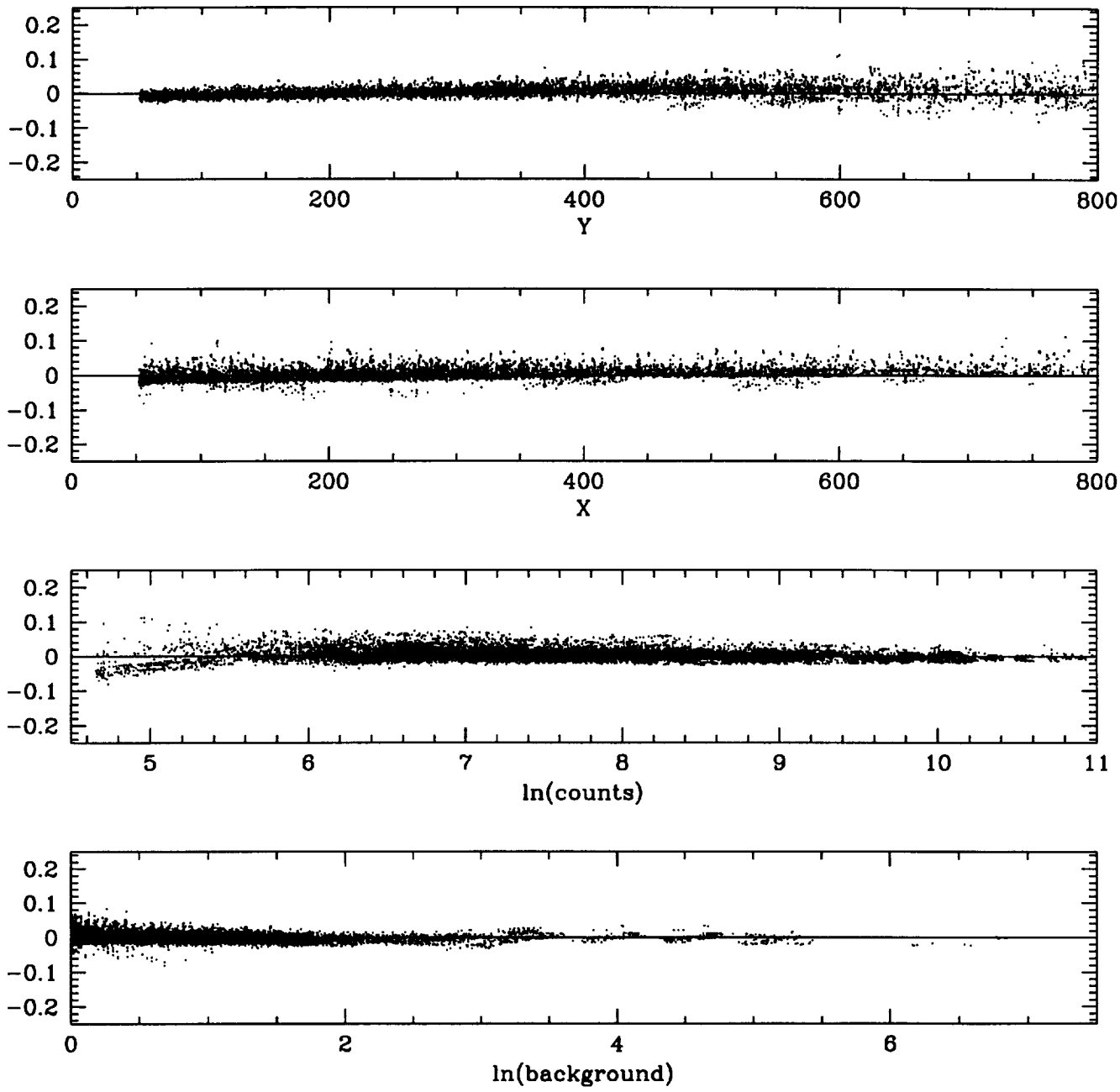

Fig. 8.— Differences in CTE and zero point corrections between S98 and the present study for cold F555W and F814W data obtained before 1997. Positive values mean that the S98 correction is larger, thus producing a smaller (brighter) corrected magnitude.

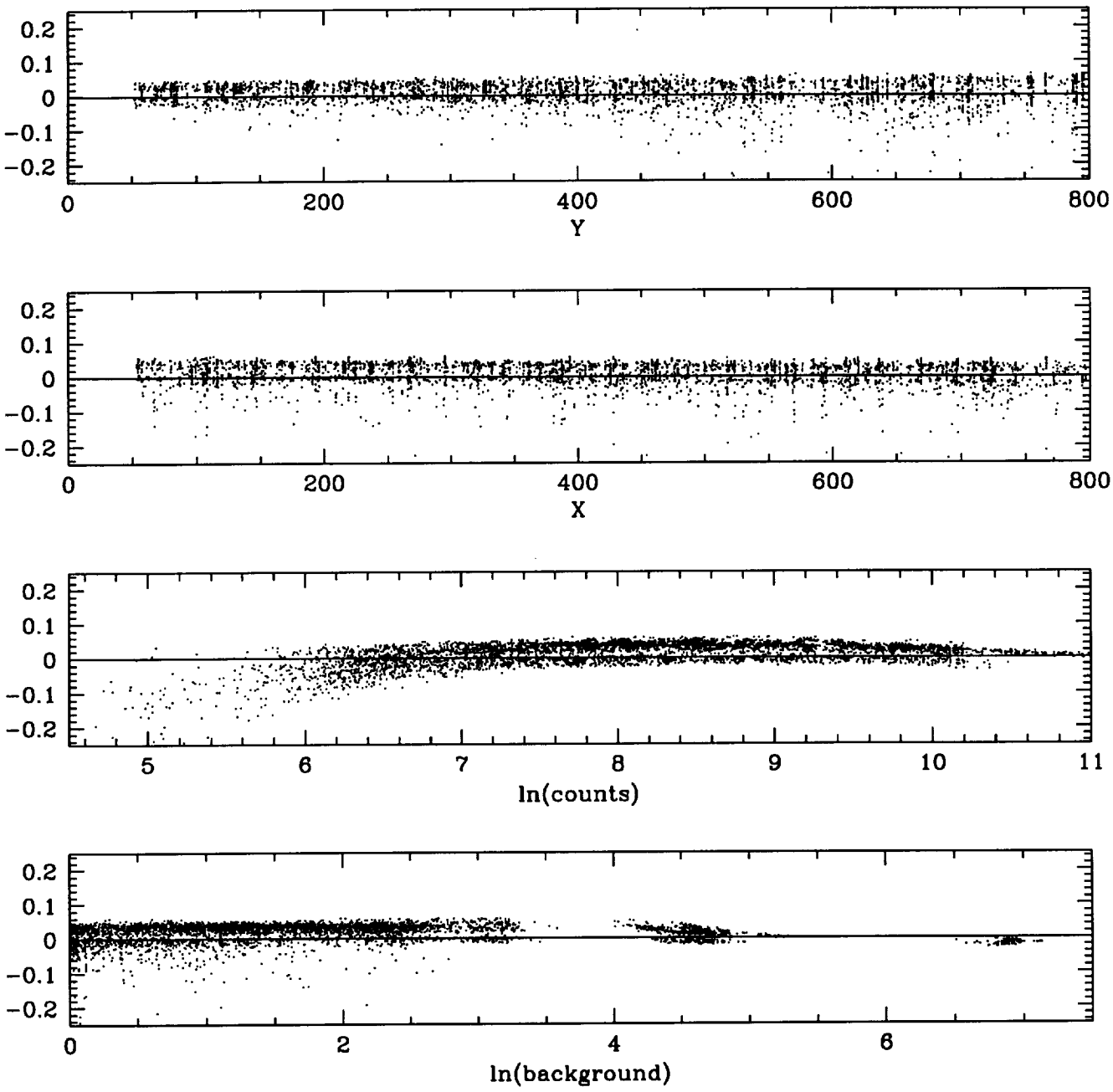

Fig. 9.— Same as Figure 8 for data obtained in 1997 and 1998, compared with SLP00

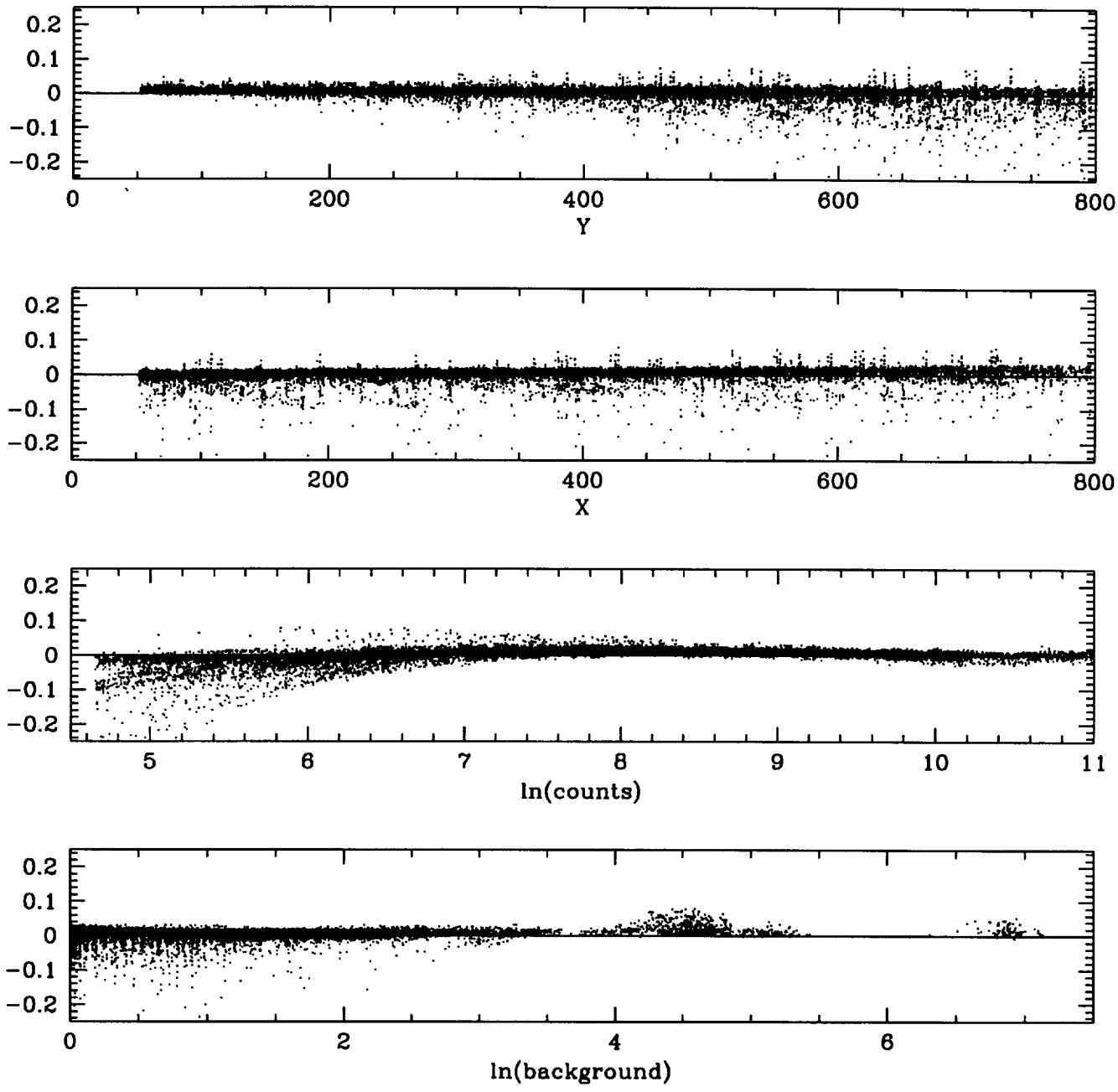

Fig. 10.— Same as Figure 8 for data cold obtained through February 1999, compared with WHC99

Table 1. Cold CTE Coefficients

c_i	Value	Description
y_0	0.018 ± 0.003	YCTE base
y_1	0.097 ± 0.005	YCTE time-independent
y_2	0.041 ± 0.002	YCTE time-dependent
y_3	0.088 ± 0.031	YCTE count-independent
y_4	0.507 ± 0.019	YCTE count-dependent
y_5	0.035 ± 0.025	YCTE background-dependent
y_6	0.042 ± 0.008	YCTE background-dependent e^{-bg}
x_1	0.024 ± 0.002	XCTE time-independent
x_2	0.002 ± 0.001	XCTE time-dependent
x_4	0.196 ± 0.042	XCTE count-dependent
x_5	0.126 ± 0.034	XCTE background-dependent

Table 2. Warm CTE Coefficients

c_i	Value	Description
y_0	0.103 ± 0.003	YCTE base
y_1	0.028 ± 0.004	YCTE count-dependent constant
y_2	0.959 ± 0.089	YCTE count dependence

Table 3. Color and Temperature Corrections

Color	Cold ΔZP_{color}	Warm ΔZP_{color}
U[1]	-0.023 ± 0.010	0.045 ± 0.010
B	-0.016 ± 0.001	0.034 ± 0.002
V	-0.009 ± 0.001	0.013 ± 0.001
R	-0.007 ± 0.001	0.013 ± 0.002
I	0.012 ± 0.001	-0.014 ± 0.001

[1]U zero point corrections are extrapolated from the other four colors.

Table 4. Zero Point Corrections for Non-Standard Filters

Filter	Standard	ΔZP_{filter}
F380W	F336W	-0.084 ± 0.004
F410M	F439W	-0.055 ± 0.006
F450W	F439W	0.006 ± 0.004
F467M	F439W	0.062 ± 0.004
F547M	F555W	0.005 ± 0.003
F569W	F555W	0.017 ± 0.002
F606W	F555W	0.019 ± 0.002
F622W	F675W	0.006 ± 0.007
F702W	F675W	-0.010 ± 0.002
F785LP	F814W	-0.008 ± 0.003
F791W	F814W	0.026 ± 0.005
F850LP	F814W	0.001 ± 0.005
F1042M	F814W	0.004 ± 0.006

Table 5. ΔZ_{CG} Values

Chip	gain=14	gain=7
PC1	-0.044 ± 0.001	0.701 ± 0.001
WFC2	0.007 ± 0.000	0.761 ± 0.000
WFC3	-0.007 ± 0.000	0.749 ± 0.000
WFC4	-0.005 ± 0.000	0.722 ± 0.000

Table 6. New Flight System Zero Points

Filter	Cold Z_{FG}	Warm Z_{FG}
F336W	18.528 ± 0.010	18.460 ± 0.010
F380W	20.218 ± 0.004	20.169 ± 0.005
F410M	18.576 ± 0.007	18.527 ± 0.007
F439W	20.086 ± 0.001	20.036 ± 0.002
F450W	21.183 ± 0.004	21.133 ± 0.005
F467M	19.114 ± 0.004	19.065 ± 0.004
F547M	20.843 ± 0.003	20.820 ± 0.003
F555W	21.734 ± 0.001	21.712 ± 0.001
F569W	21.411 ± 0.003	21.389 ± 0.003
F606W	22.075 ± 0.002	22.052 ± 0.002
F622W	21.544 ± 0.007	21.525 ± 0.007
F675W	21.241 ± 0.001	21.221 ± 0.002
F702W	21.645 ± 0.002	21.626 ± 0.003
F785LP	19.873 ± 0.003	19.899 ± 0.003
F791W	20.669 ± 0.005	20.695 ± 0.005
F814W	20.827 ± 0.001	20.853 ± 0.001
F850LP	19.126 ± 0.005	19.153 ± 0.005
F1042M	15.351 ± 0.006	15.378 ± 0.006

Table 7. New Transformations

Filter	SMAG	SCOL	T_1	T_2	$Z_{FS,cold}$	$Z_{FS,warm}$	C_{min}	C_{max}
F300W	U	(U-B)	-1.532	-0.519	18.156	18.144		-0.2
F300W	U	(U-B)	-0.427	0.138	18.181	18.169	0.2	1.0
F336W	U	(U-B)	-0.844	-0.160	18.528	18.460		
F336W	U	(U-V)	-0.240	0.048	18.787	18.719		
F336W	U	(U-R)	-0.172	0.041	18.820	18.752		
F336W	U	(U-I)	-0.149	0.038	18.840	18.772		
F380W	B	(B-V)	-0.581	0.777	20.243	20.194		0.5
F380W	B	(B-V)	-0.943	0.103	20.595	20.546	0.5	1.4
F410M	B	(B-V)	-0.183	-0.287	18.886	18.837		1.4
F439W	B	(U-B)	-0.103	-0.046	20.073	20.023		
F439W	B	(B-V)	0.003	-0.088	20.086	20.036		
F439W	B	(B-R)	0.019	-0.049	20.080	20.030		
F439W	B	(B-I)	0.005	-0.023	20.083	20.033		
F450W	B	(B-V)	0.230	-0.003	21.185	21.135		1.4
F467M	B	(B-V)	0.480	-0.299	19.121	19.072		0.5
F467M	B	(B-V)	0.432	-0.002	19.072	19.023	0.5	1.4
F547M	V	(V-I)	0.027	-0.032	20.838	20.815		1.1
F547M	V	(V-I)	0.049	-0.013	20.790	20.767	1.1	
F555W	V	(U-V)	-0.014	0.005	21.715	21.693		
F555W	V	(B-V)	-0.060	0.033	21.734	21.712		
F555W	V	(V-R)	-0.121	0.120	21.739	21.717		
F555W	V	(V-I)	-0.052	0.027	21.734	21.712		
F569W	V	(V-I)	0.089	-0.003	21.409	21.387		2.0
F569W	V	(V-I)	-0.125	0.022	21.741	21.719	2.0	
F606W	V	(V-I)	0.254	0.012	22.084	22.061		2.0
F606W	V	(V-I)	-0.247	0.065	22.874	22.851	2.0	
F622W	R	(V-R)	-0.252	-0.111	21.558	21.539		
F675W	R	(U-R)	0.039	-0.007	21.261	21.241		
F675W	R	(B-R)	0.092	-0.017	21.242	21.222		
F675W	R	(V-R)	0.253	-0.125	21.241	21.221		
F675W	R	(R-I)	0.273	-0.066	21.232	21.212		
F702W	R	(V-R)	0.343	-0.177	21.650	21.631		0.6
F702W	R	(V-R)	0.486	-0.079	21.528	21.509	0.6	
F785LP	I	(V-I)	0.091	0.020	19.876	19.902		

Table 7—Continued

Filter	SMAG	SCOL	T_1	T_2	$Z_{FS,cold}$	$Z_{FS,warm}$	C_{min}	C_{max}
F791W	I	(V-I)	-0.029	-0.004	20.669	20.695		1.0
F791W	I	(V-I)	-0.084	0.011	20.710	20.736	1.0	
F814W	I	(U-I)	-0.018	0.002	20.803	20.829		
F814W	I	(B-I)	-0.031	0.007	20.823	20.849		
F814W	I	(V-I)	-0.062	0.025	20.827	20.853		
F814W	I	(R-I)	-0.112	0.084	20.827	20.853		
F850LP	I	(V-I)	0.160	0.023	19.108	19.135		
F1042M	I	(V-I)	0.350	0.022	15.298	15.325		

Table 8. Second-Order Residuals after Correction

	$bg < 100$	$bg > 100$	$ct < 2000$	$ct > 2000$
$ct < 2000$	0.003 ± 0.001	-0.003 ± 0.005		
$ct > 2000$	-0.001 ± 0.001	-0.008 ± 0.003		
$yr < 1996$	0.001 ± 0.001	-0.010 ± 0.007	0.004 ± 0.001	-0.001 ± 0.001
$yr > 1996$	0.000 ± 0.001	-0.006 ± 0.002	0.001 ± 0.001	-0.001 ± 0.001

Table 9. Residuals From Four CTE and Zero Point Correction Systems

Year	Npoints	S98	WHC99	SLP00	Present Work
all	28221	0.031 ± 0.103	-0.009 ± 0.092	0.010 ± 0.099	-0.001 ± 0.089
1994	6504	0.010 ± 0.105	-0.008 ± 0.106	-0.018 ± 0.108	-0.001 ± 0.104
1995	6917	0.019 ± 0.097	-0.003 ± 0.092	-0.011 ± 0.093	0.003 ± 0.089
1996	2003	0.015 ± 0.069	-0.018 ± 0.064	0.005 ± 0.067	-0.005 ± 0.064
1997	3436	0.030 ± 0.085	-0.008 ± 0.080	0.029 ± 0.083	0.002 ± 0.079
1998	1956	0.044 ± 0.092	-0.014 ± 0.085	0.022 ± 0.087	-0.007 ± 0.082
1999	4259	0.066 ± 0.112	-0.008 ± 0.096	0.040 ± 0.103	0.002 ± 0.089
2000	3146	0.065 ± 0.105	-0.018 ± 0.089	0.040 ± 0.096	-0.004 ± 0.082